Journal of the Korean Nuclear Society
Volume 32, Number 4, pp.410~423, August 2000

Two Dimensional Analysis for the External Vessel Cooling Experiment

Ho-Jun Yoon and Kune Y. Suh
Seoul National University
San 56-1 Shinrim-dong, Kwanak-gu, Seoul, 151-742, Korea
kysuh@plaza.snu.ac.kr

(Received May 15, 2000)

Abstract

A two-dimensional numerical model is developed and applied to the LAVA-EXV tests performed at the Korea Atomic Energy Research Institute (KAERI) to investigate the external cooling effect on the thermal margin to failure of a reactor pressure vessel (RPV) during a severe accident. The computational program was written to predict the temperature profile of a two-dimensional spherical vessel segment accounting for the conjugate heat transfer mechanisms of conduction through the debris and the vessel, natural convection within the molten debris pool, and the possible ablation of the vessel wall in contact with the high temperature melt. Results of the sensitivity analysis and comparison with the LAVA-EXV test data indicated that the developed computational tool carries a high potential for simulating the thermal behavior of the RPV during a core melt relocation accident. It is concluded that the main factors affecting the RPV failure are the natural convection within the debris pool and the ablation of the metal vessel. The simplistic natural convection model adopted in the computational program partly made up for the absence of the mechanistic momentum consideration in this study. Uncertainties in the prediction will be reduced when the natural convection and ablation phenomena are more rigorously dealt with in the code, and if more accurate initial and time-dependent conditions are supplied from the test in terms of material composition and its associated thermophysical properties.

Key Words : severe accident, core melt, external vessel cooling, ADI method, natural convection, ablation, COASISO, LAVA-EXV

1. Introduction

A severe accident may arise from core uncovery in the pressurized water reactor (PWR) when the core does not adequately get cooled by the coolant. The melted core may then be relocated into the reactor pressure vessel (RPV) lower head. As the melting temperature of the

RPV may be lower than the temperature of the overheated core material, the RPV may melt unless proper severe accident mitigation strategies are at hand. One of those candidate strategies is the external cooling of the RPV lower head. The LAVA-EXV experiments [1] were performed at the Korea Atomic Energy Research Institute (KAERI) to investigate the external cooling effect on the thermal margin to failure of a RPV during a severe accident. Also, a number of investigations were performed for the external cooling of the lower head as summarized below.

O' Brien and Hawkes [2] performed a thermal analysis to assess the viability of external water flooding as a cooling strategy to prevent RPV thermal failure during a severe accident with partial core melting and relocation to the lower head. For the molten pool in the lower head, the turbulent natural convection heat flux distribution predicted from the FIDAP simulation was used to determine the RPV wall temperature. Vessel wall temperatures and heat fluxes were obtained over a range of decay heat values using a one-dimensional heat conduction model. It was concluded that if the turbulent natural convection heat transfer coefficients predicted from the numerical simulation are correct, thermal failure of the vessel wall would occur.

Park and Dhir [3] investigated the effectiveness of flooding the cavity of a PWR in preventing the RPV melt-through. Two-dimensional transient and steady state analyses were carried out including the heat loss by radiation to the upper regions of the RPV and the unwetted portion of the lower head. The effect of internal circulation in the molten core material on heat transfer at the bounding walls was determined by extending the correlations used in their study. Radiative heat transfer from the molten pool to surrounding structures was also included in their analysis. They concluded that remelting of the crust would occur after heat up of the pool. The effects of the emissivities of the pool free surface, the structure, and the structure temperature on the RPV inner wall were predicted to be small when the Mayinger et al. correlation [4] was used.

Henry et al. [5] performed the experiment to demonstrate that nucleate boiling is the dominant heat removal process from the outer surface of a simulated RPV lower head surrounded by typical reflective insulation used in the nuclear power plant. Their experiment showed that heat fluxes approaching $1MW/m^2$ could be removed by boiling on the outer surface even with the vessel insulated. No indications of high wall surface temperatures were observed. They insisted that the entire transient was characterized by nucleate boiling and the lower head could effectively remove the energy transferred to the wall through the debris crust.

The literature survey appears to indicate that the in-vessel retention can be achieved by full flooding of the reactor cavity to cool the external wall of the lower head thereby avoiding a structural failure by creep rupture or melt-through. However, application of this approach to large power reactors is not trivial because of relatively short time between the detection of core melting and the lower head failure and worse, the time it takes to flood the spacious reactor cavity with generally limited openings for water injection. Therefore, special design features to facilitate rapid flooding are essential to the success of the in-vessel retention. In this study we have analytically examined the thermal behavior of a vessel containing the exceedingly high temperature melt. An improved in-vessel retention method utilizing hemispherical shell gap structures called the COASISO (Corium Attack Syndrome Immunization Structure

Outside) is proposed for rapid cooling of the lower head.

In the absence of comprehensive predictive method available in the literature, we developed a computational tool to examine the thermal interactions between the vessel wall and the high temperature melt in terms of conjugate heat transfer mechanisms of convection, conduction and ablation. The three factors serve the backbone in interpreting the sophisticated thermal interactions of the vessel wall with the scorching melt inside and possibly cooling water outside. Our numerical model comprises the two-dimensional solution of heat conduction through the debris and the vessel, simplistic treatment of the natural convection within the molten pool using an experimental correlation, and consideration of the potential ablation of the vessel wall by a parametric approach of changing the thermophysical properties of the emptied nodes with those of the newly filling material from above. The computed results are compared with KAERI's LAVA-EXV experimental data [1] and FLUENT calculations [6].

2. Model Description

2.1. Governing Differential Equation

In calculating the two-dimensional temperature profile in the vessel for the external and no external cooling cases we used the alternating direction implicit (ADI) method adapted from El-Genk et al. [7] for the hemispherical geometry. They used the ADI method to analyze the temperature profile in the test section and to calculate the heat flux using the temperatures of the inner and outer surfaces. As our geometry and the boundary conditions are similar to those of El-Genk et al.'s test section, we chose to employ their numerical scheme in performing the analysis. In this method temperatures are calculated implicitly alternating in r and θ directions, respectively.

A two-dimensional transient heat conduction equation in the spherical coordinates is

$$\rho c_p\left(\frac{\partial T}{\partial t}\right)=\frac{1}{r^2}\frac{\partial}{\partial r}\left(kr^2\frac{\partial T}{\partial r}\right)+\frac{1}{r^2\sin\theta}\frac{\partial}{\partial\theta}\left(k\sin\theta\frac{\partial T}{\partial\theta}\right) \quad (1)$$

The diffusion terms in equation (1) were discretized and split into two parts. The whole solution was obtained in two steps. In the first step the diffusion terms in the θ direction were represented implicitly, while those in the r direction were explicit:

$$\rho_v c_{p_v}\Delta V_{v_{i,j}}\frac{T^*_{i,j}-T^n_{i,j}}{\Delta t/3}=k^{L}_{v_{i,j}}\frac{T^*_{i,j-1}-T^*_{i,j}}{r_i\Delta\theta}\Delta AL^v_{i,j}$$
$$+k^{R}_{v_{i,j}}\frac{T^*_{i,j+1}-T^*_{i,j}}{r_i\Delta\theta}\Delta AR^v_{i,j}+k^{U}_{v_{i,j}}\frac{T^n_{i+1,j}-T^n_{i,j}}{\Delta r}\Delta AU^v_{i,j} \quad (2)$$
$$+k^{D}_{v_{i,j}}\frac{T^n_{i-1,j}-T^n_{i,j}}{\Delta r}\Delta AD^v_{i,j}$$

In the second step the diffusion terms in the θ direction were represented explicitly, while those in the r direction were implicit:

$$\rho_v c_{p_v}\Delta V_{v_{i,j}}\frac{T^{n+1}_{i,j}-T^*_{i,j}}{\Delta t/3}=k^{L}_{v_{i,j}}\frac{T^*_{i,j-1}-T^*_{i,j}}{r_i\Delta\theta}\Delta AL^v_{i,j}$$
$$+k^{R}_{v_{i,j}}\frac{T^*_{i,j+1}-T^*_{i,j}}{r_i\Delta\theta}\Delta AR^v_{i,j}+k^{U}_{v_{i,j}}\frac{T^{n+1}_{i+1,j}-T^{n+1}_{i,j}}{\Delta r}\Delta AU^v_{i,j} \quad (3)$$
$$+k^{D}_{v_{i,j}}\frac{T^{n+1}_{i-1,j}-T^{n+1}_{i,j}}{\Delta r}\Delta AD^v_{i,j}$$

where T^n and T^{n+1} are the temperatures at the previous and present time steps, respectively, and T^* is the intermediate time step value. More detailed discretized forms of the differential equations for the respective regions for the first step of the ADI method follow:

Vessel outer surface

$$\rho_v c_{p_v} \Delta V_{v_{i,j}} \frac{T^*_{i,j} - T^n_{i,j}}{\Delta t/3} = k^{\,L}_{v\,i,j} \frac{T^*_{i,j-1} - T^*_{i,j}}{r_i \Delta\theta} \Delta AL^v_{i,j}$$

$$+ k^{\,R}_{v\,i,j} \frac{T^*_{i,j+1} - T^*_{i,j}}{r_i \Delta\theta} \Delta AR^v_{i,j} + k^{\,U}_{v\,i,j} \frac{T^n_{2,j} - T^n_{1,j}}{\Delta r} \Delta AU^v_{i,j} \quad (4)$$

$$+ h\left(T_{bulk} - T^n_{1,j}\right) \Delta AD^v_{i,j}$$

Vessel inner surface

$$\rho_v c_{p_v} \Delta V_{v_{i,j}} \frac{T^*_{i,j} - T^n_{i,j}}{\Delta t/3} + \rho_m c_{p_m} \Delta V_{m_{i,j}} \frac{T^*_{i,j} - T^n_{i,j}}{\Delta t/3}$$

$$= k^{\,L}_{v\,i,j} \frac{T^*_{i,j-1} - T^*_{i,j}}{r_i \Delta\theta} \Delta AL^v_{i,j} + k^{\,R}_{v\,i,j} \frac{T^*_{i,j+1} - T^*_{i,j}}{r_i \Delta\theta} \Delta AR^v_{i,j}$$

$$+ k^{\,U}_{v\,i,j} \frac{T^n_{i+1,j} - T^n_{i,j}}{\Delta r} \Delta AU^v_{i,j} + k^{\,D}_{v\,i,j} \frac{T^n_{i-1,j} - T^n_{i,j}}{\Delta r} \Delta AD^v_{i,j} \quad (5)$$

$$+ k^{\,L}_{m\,i,j} \frac{T^*_{i,j-1} - T^*_{i,j}}{r_i \Delta\theta} \Delta AL^m_{i,j} + k^{\,R}_{m\,i,j} \frac{T^*_{i,j+1} - T^*_{i,j}}{r_i \Delta\theta} \Delta AR^m_{i,j}$$

$$+ k^{\,U}_{m\,i,j} \frac{T^n_{i+1,j} - T^n_{i,j}}{\Delta r} \Delta AU^m_{i,j} + k^{\,D}_{m\,i,j} \frac{T^n_{i-1,j} - T^n_{i,j}}{\Delta r} \Delta AD^m_{i,j}$$

Upper surface of the molten material

$$\rho_m c_{p_m} \Delta V_{m_{i,j}} \frac{T^*_{i,j} - T^n_{i,j}}{\Delta t/3} = k^{\,L}_{m\,i,j} \frac{T^*_{i,j-1} - T^*_{i,j}}{r_i \Delta\theta} \Delta AL^m_{i,j}$$

$$+ k^{\,R}_{m\,i,j} \frac{T^*_{i,j+1} - T^*_{i,j}}{r_i \Delta\theta} \Delta AR^m_{i,j} + \varepsilon\sigma\left(T^4_{air} - T^{n\,4}_{i,j}\right) \Delta AU^m_{i,j} \quad (6)$$

$$+ k^{\,D}_{m\,i,j} \frac{T^n_{i-1,j} - T^n_{i,j}}{\Delta r} \Delta AD^m_{i,j}$$

2.2. Natural Convection in the Molten Pool

This code basically calculates the temperature of the vessel and the molten material using a two-dimensional conduction equation. A natural convection model was introduced between the first step and the second step of the ADI scheme.

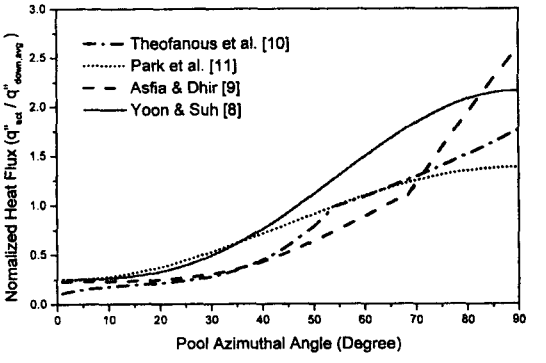

Fig. 1. Comparison of Natural Convection Correlations for the Pool

After the first step calculation, we obtain the temperatures for all the nodes. There were solid state nodes and liquid state nodes. To account for natural convection, we first sum the heat transfer rate from the liquid state nodes to solid state nodes using the known temperatures for all the interfacing nodes. We then obtain the average heat flux by dividing the total heat transfer by the interface area between the liquid and solid nodes. It is generally believed that the azimuthal heat flux distribution is governed by natural convection within the molten pool. In this study, we adopt the heat transfer coefficients varying with the local position along the vessel azimuthal angle. Several investigators proposed correlations based on the experimental data, some of which are collected in Fig. 1.

Yoon and Suh [8] observed that the relevant correlations [9-12] share essentially the same trend except that Park et al.' s correlation [11] and Suh and Henry' s correlation [12] did not fit the experimental data of Jahn and Reineke' s [13] adequately. As shown in Fig. 2, Yoon and Suh [8] modified Suh and Henry' s correlation [12] based on the experimental data [13] as

$$\frac{h(\theta)}{h_{down}} = C_\theta + \left(\frac{12(1 - C_\theta)(1 - \cos\phi)}{3(\phi - \cos\phi\sin\phi) - 2\sin^3\phi\cos\phi}\right) \times \sin^3\theta \quad (7)$$

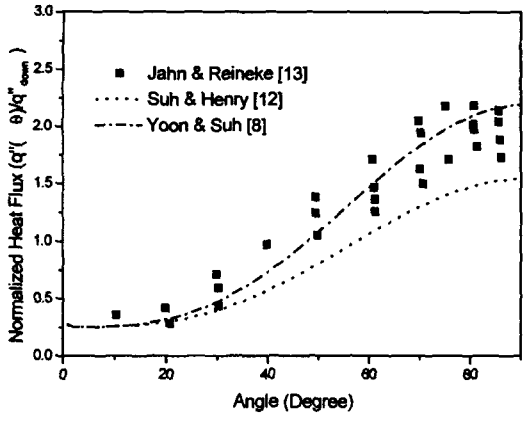

Fig. 2. New Fitting Correlation for the Data of Jahn and Reineke' s Experiment

where C_ϕ= 0.25, and ϕ is the polar angle at the pool surface.

Using the azimuthal heat flux and a one-dimensional heat conduction equation, we updated the temperatures for the solid state nodes, test vessel and the solidified crust. The one-dimensional heat conduction equation was numerically solved implicitly for the r direction. During this step the temperatures for all the nodes were redistributed in the third step. Using this method, we could approximate the natural convection effect during the temperature calculation process.

2.3. Ablation of the Vessel Wall

The molten core material will be relocated into the lower head vessel during a severe accident. In this case the temperature of the falling molten core material will be higher than the melting temperature of the vessel. In addition, as the core material carries the decay heat, the temperature of the vessel will soar. If the molten core material is not cooled enough for whatever the reason, and if there is no external cooling, the temperature of the vessel will exceed the melting point at the inner surface. The molten part of the vessel will be detached from the vessel body. To model this phenomenon, we adopted an approximating method.

The first method for modeling ablation was that the vacant space after melting of the vessel was replaced by the adjacent core material above the vanished vessel node. Thus the material properties and temperature of the vacant node of the vessel were replaced with those of the overlying core material. The second method presumed that the temperature of the core material filling the vacant space was higher than the melting temperature of the solidified core material overlying the vacant node. Due to the density difference between the core material and the vessel and the natural convection in the molten pool, the vacant space will be filled with the liquid core material through the crack of the solid crust of the core material.

Figure 3 presents the flow chart for the whole computational procedure following which the conjugate mechanisms of two-dimensional heat conduction (r and θ A), azimuthal natural convection (θ only) and node-wise ablation are

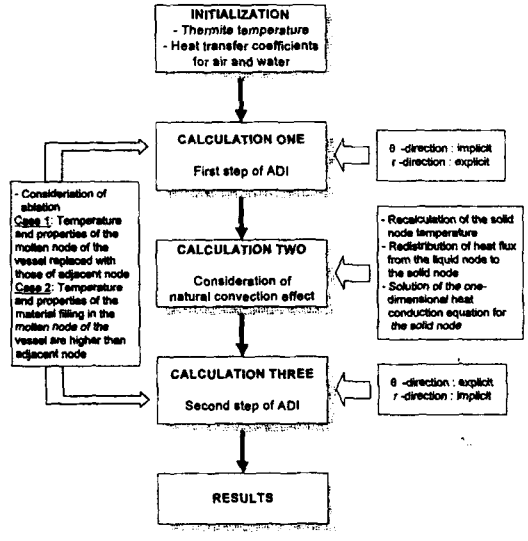

Fig. 3. Flow Chart for Calculation Sequence of Thermal Interactions

treated to simulate rather complicated thermal interactions between the debris and the vessel.

3. Description of the LAVA-EXV Experiment

To validate results from the computational program, we compared the calculated data with test data from the LAVA-EXV vessel shown in Fig. 4.

The vessel inner diameter was 0.5m and the thickness was 0.025m. The thermite mass was 40kg. The LAVA-EXV experiments were divided into three parts. The first one was the dry experiment. This experiment was performed without external cooling in the open atmosphere. The second and third ones were the external water cooled experiments. The second was the forced convection boiling experiment, while the third was the pool boiling experiment at 16atm. For the external cooling, a hemispherical shell structure was placed underneath the vessel with 0.025m gap. For the second experiment, the water was injected through the 0.025m pipe into the gap of 0.025m. The pool boiling experiment was performed in the gap filled with water. There was no supplement of water during the test. The physical properties were taken from the LAVA-EXV experiment. In calculating the temperature profile, one of the most important factors was the initial temperature of the thermite. Generally the thermite reaction is quite exothermic. If the exothermic energy were to be calorimetrically converted to temperature, the temperature will reach a neighborhood of 3497K. Because of its high temperature, the surface radiative emission to the surroundings is extremely high. Unfortunately, however, no information was available for the thermite temperature history from the experiment. We thus assumed the initial temperature of the thermite to be 2700K and 3400K, consistently with KAERI's initialization in the FLUENT analysis [6], in performing the sensitivity analyses.

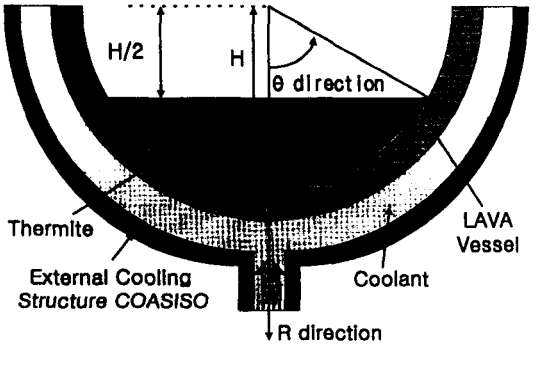

Fig. 4. Test Vessel of the LAVA-EXV Experiment

4. Results and Discussion

4.1. Uncertainties in the Current Model

During the course of this work it was felt that uncertainties exist in the current numerical model so that accurate treatment of this rather complex thermal and material interactions of the high temperature melt compound and the vessel indeed calls for mechanistic models for the multi-component, multi-phase, turbulent natural convection and solidification of the melt and for the ablation of the metallic vessel.

A two-region continuum debris model as developed by Suh and Henry [12] may be adopted and expanded to characterize the debris material and heat transport in the lower plenum under severe accident conditions. In this model the debris bed is conglomerated into the oxidic pool and an overlying metallic layer. Debris crusts can develop on three surfaces: the top of the molten pool, the RPV wall, and the lower plenum structures. The crust temperature profile is assumed to be parabolic accounting for the decay heat generation. The oxidic debris pool is homogeneously mixed and has the same material

composition, and hence the same thermophysical properties as the crusts. The metallic constituents are assumed to rise to the top of the debris pool. Steady-state relationships are used to describe the heat transfer rates, with the assessment of solid or liquid state, and the liquid superheat in the pool being based on the average debris temperature. Natural convection heat transfer from the molten debris pool to the upper, lower and embedded crusts is calculated based on the pool Rayleigh number. The conduction heat transfer from the crusts is computed by the crust temperature profile. The downward heat flux is transferred to the lower part of the RPV lower head through a crust-to-RPV contact resistance. The sideward heat flux is transferred to the upper regions of the RPV lower head as well as the internal structures. The upward heat flux goes to the metal layer, particulated debris, water, or structures above. If the RPV were to be externally submerged, the heat removal is enhanced by the ex-vessel cooling due to nucleate boiling.

4.2. Comparison with the FLUENT Results

In this section we present results of the LAVA-EXV analysis using the predictive tool in comparison to the FLUENT calculations [6] for the same problem. They assumed that the thermite part was pure Fe and the initial temperature of Fe was 2700K and 3400K. The analysis was performed for the dry experiment assuming the heat transfer coefficient of the air of 50W/m^{2}K and the melting temperature of the vessel of 1700K. At this point we do not intend to validate one computational result versus the other from the technical rigor point of view. Rather we attempt to shed light on the similarities and differences between the two code calculations, gain insight into the uncertain areas of the problem at hand, and further explore possible solutions to the issues requiring further attention.

The FLUENT 4.32 code [14] predicts detailed transient two-dimensional thermal and flow distributions by solving the conservation equations for mass, momentum and energy using a control volume based finite difference method. The unsteady turbulent two-dimensional basic equations for natural convection and heat transfer are solved using the SIMPLE algorithm and the power-law scheme in the curvilinear coordinates.

Due to lack of the ablation model for the vessel wall in the FLUENT code, however, we chose to compare the results without considering the ablation. Considering uncertainties in the material composition and its associated thermophysical properties, our results showed similar trends in fair agreement with the FLUENT results. The timing of the vessel heatup and the eventual failure lagged the FLUENT results by several seconds as may be inferred from Figs. 5 and 6, however. According to the natural convection effect, the peak temperature occurred at the similar azimuthal location (i.e., θ = 50°) in the FLUENT and our results. The difference in the two codes' predictions for the azimuthal temperature profile may be attributed to consideration of the buoyancy driven natural convection flow in FLUENT versus simple application of the Yoon and Suh correlation [8] in our code. Another factor in explaining the difference in the vessel behavior including its failure time is the difficulty in obtaining accurate material compositions and properties (both initial and time-dependent conditions) for the debris used in the tests. Compared to our predictions, the results of FLUENT showed faster heatup and thus failure of the vessel given the same initial conditions. As both FLUENT and our program were applied to the dry case (i.e., atmospheric, no external vessel cooling water) no major differences were readily detectable from the heat removal rate on the outer

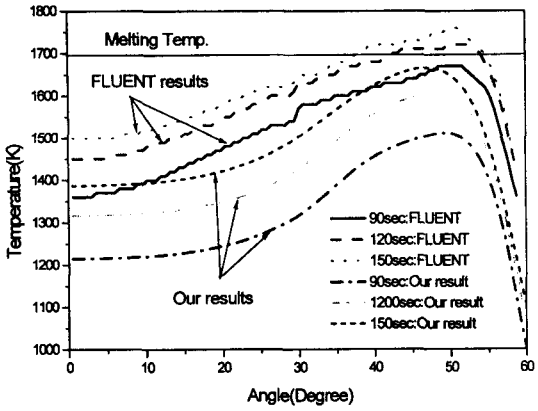

Fig. 5. Azimuthal Temperature Distribution (Initial Temp. = 2700K)

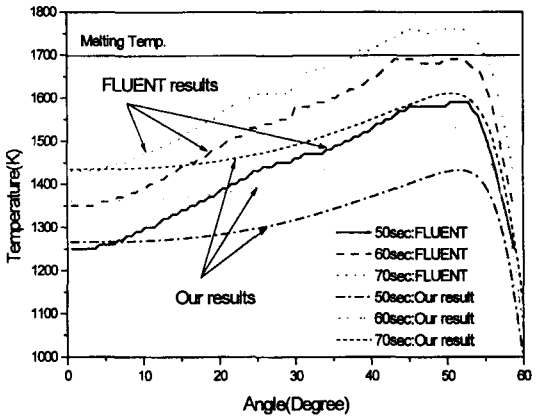

Fig. 6. Azimuthal Temperature Distribution (Initial Temp. = 3400K)

surface of the vessel. It is thus seen that our two-dimensional program essentially yields reasonable results for the thermal behavior of the vessel being attacked by the high temperature melt.

4.3. Sensitivity Analysis

For the sensitivity analysis of our two-dimensional code, we chose the following test factors:

- initial temperature of the thermite [K]: 2700, 3400
- melting temperature of the thermite [K]: 1700, 2300
- effect of the ablation model: none, first model, second model

All the sensitivity analyses were performed for the dry case. We assumed that the melting temperature of the vessel wall was 1800K rather than 1700K assumed at KAERI.

The first sensitivity analysis was performed for the melting temperature of the thermite. Since the thermite after ignition was a mixture consisting of Fe and Al_2O_3, we could not precisely determine the melting temperature of the thermite. As the melting temperature of Fe is 1700K and that of Al_2O_3 is 2300K, we chose those two temperatures for the sensitivity analysis in Fig. 7. The sensitivity analysis was performed without considering the ablation given the initial temperature of 2700K. Figure 7 presents the azimuthal temperature distribution of the outer surface for the first sensitivity analysis. The melting temperature of the thermite affects the crust thickness (the thickness of the solidified material) and finally the temperature profile of the vessel wall. It is observed that if the melting temperature of the molten material was high, the molten material is solidified more easily. Consequently, the natural convection effect on the vessel wall diminishes by means of the thicker crust.

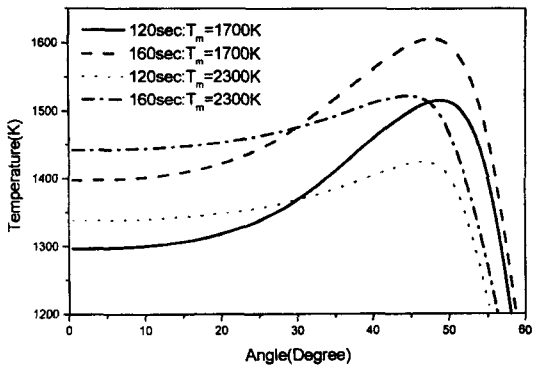

Fig. 7. Sensitivity Analysis for the Melting Temperature of Thermite

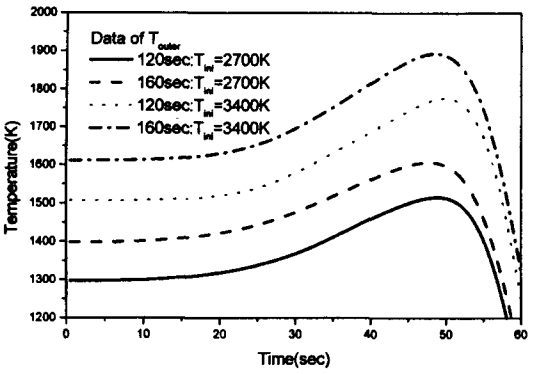

Fig. 8. Sensitivity Analysis for the Initial Temperature of Thermite

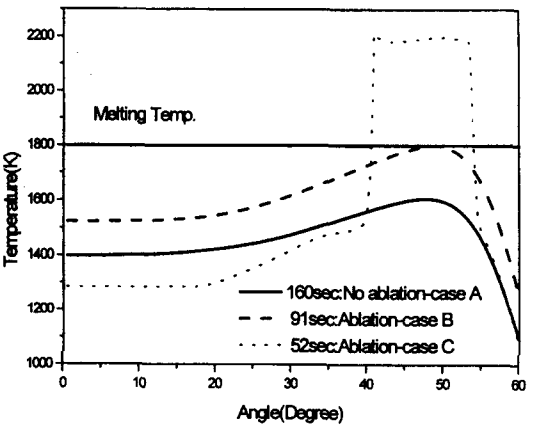

Fig. 9. Sensitivity Analysis for the Ablation Model

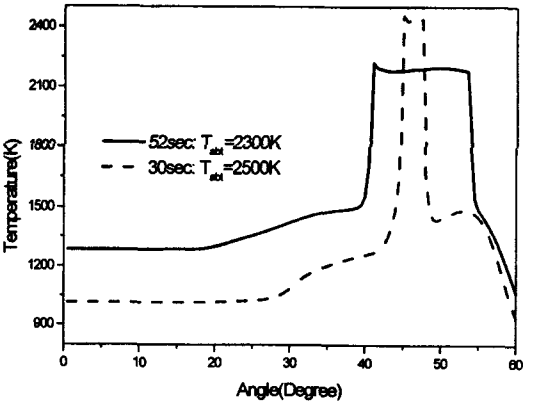

Fig. 10. Effect of Temperature of the Molten Material Occupying the Vacant Space

The second sensitivity analysis was performed for the initial temperature of the thermite. In this sensitivity study, the ablation model was not considered. The melting temperature of the thermite was assumed to be 1700K to maximize the natural convection effect. Figure 8 suggests that the dominant factor determining the failure time of the vessel was the initial temperature of the molten material as long as the ablation is not considered.

For the third sensitivity analysis, we investigated the effect of the ablation. Results of the ablation are divided into two parts as previously explained. It was assumed that the initial and melting temperatures of the molten material were 3400K and 1700K, respectively. For the second ablation model, we assumed that the temperature of the molten material occupying the vacant nodes of the vessel wall was 2300K. Figure 9 illustrates the effectiveness of the ablation model. Cases A, B and C respectively represent no ablation, the first ablation and the second ablation models. It is suggested that the main factors in determining the failure of the vessel are the ablation and the temperature of the molten material occupying the vacant space. To determine the dependency of the temperature of the molten material occupying the vacant space, we utilized the values of 2300K and 2500K, as compared in Fig. 10. Obviously, the failure time of the vessel was strongly dependent on the ablation temperature, T_{abt}. As we obtained the result at the time step of 1 sec though the calculation time was 0.01 sec, the molten area of the vessel was expanded for 1 sec so that the result for the 2300K showed different shape compared with the case of 2500K. It was observed that the earliest melting region was around 45 degrees from the bottom of the vessel. Since the whole purpose of this sensitivity analysis was to figure out how much time could be shortened for the melt-

through of the vessel by employing a simple ablation model, there was no need to pick out the curves at the same time of the test.

4.4. Application to the LAVA-EXV Experiment

We compared the numerical result with data from the LAVA-EXV experiments. In the experiments, the thermocouples were located at 2 mm and 19 mm from the outer vessel surface for the dry case and 2 mm and 12 mm from the outer vessel surface for the wet case as shown in Fig. 11. In the dry case experiment, the vessel failed 28 sec after ignition of the thermite at the location of 30°. In the experiment, the heat flux was estimated from the thermocouple readings at the locations of 0° and 15° by pair. Of the two locations, we chose the location of 15°. According to Fig. 12, the failure at 15° is predicted to occur at 45 sec. The first failure occurred in the region between 45° and 50° by means of the natural convection and the ablation effect at 30 sec in our calculation.

For the forced convection boiling, we investigated the azimuthal temperature variation of the outer surface and the temperature profiles at 15 o with the heat transfer coefficients of 10000 W/m^2K and 5000 W/m^2K, respectively. Here the choice of the value for the heat transfer coefficient is purely from the sensitivity study point of view so that no physical explanations deserve the credit. According to Fig. 13, both cases showed similar trends but the temperatures were different apparently because of the different heat transfer coefficients applied at the outer vessel boundary.

In fact the heat transfer coefficient would be different along the angular position. As there were no directly applicable data available for the heat transfer coefficient at the downward facing hemispherical wall, we chose the constant value spanning the whole bottom surface area. When

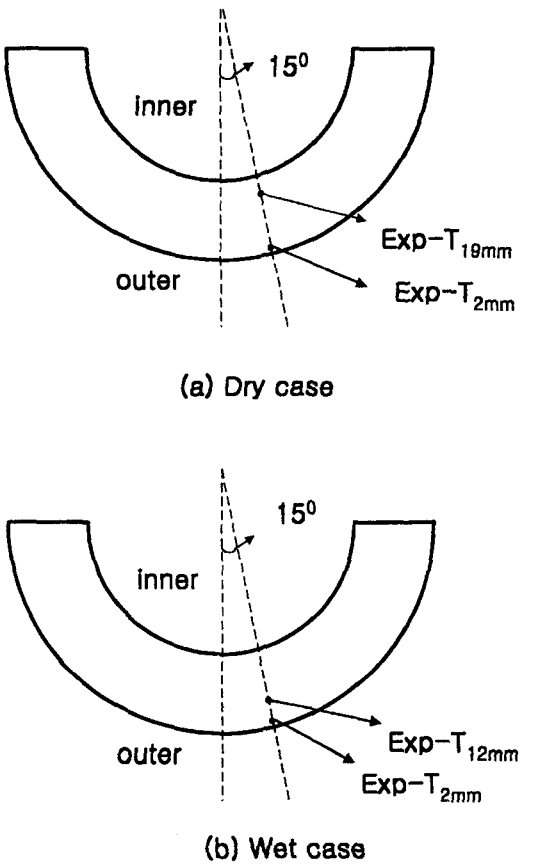

Fig. 11. Location of Thermocouples in LAVA-EXV Test Vessels

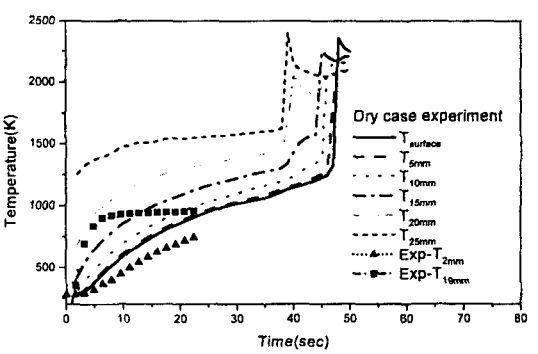

Fig. 12. Temperature History in Dry Experiment

we compared the results with the test data for the case of forced convection boiling of the LAVA-

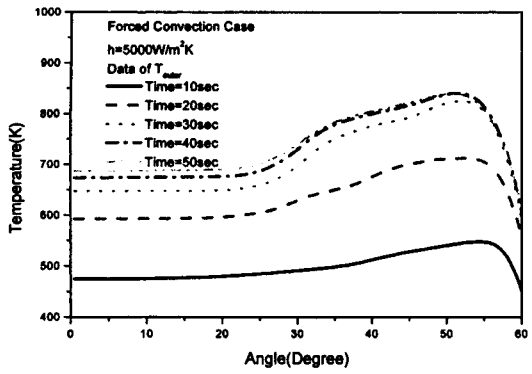

(a) h=5000 W/m²K

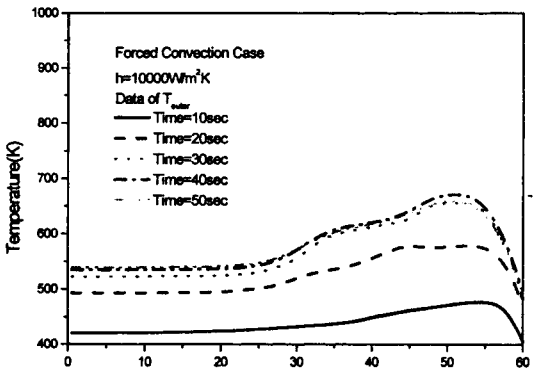

(b) h=10000 W/m²K

Fig. 13. Azimuthal Temperature Variation with Time for Forced Convective Boiling

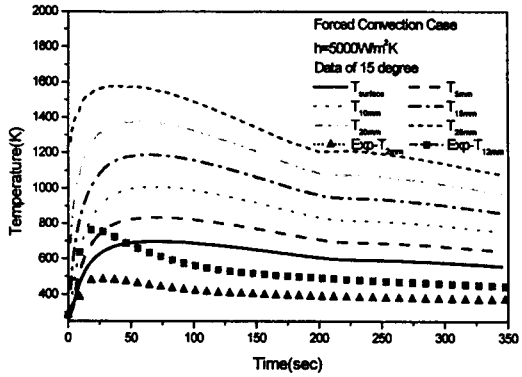

(a) h=5000 W/m²K

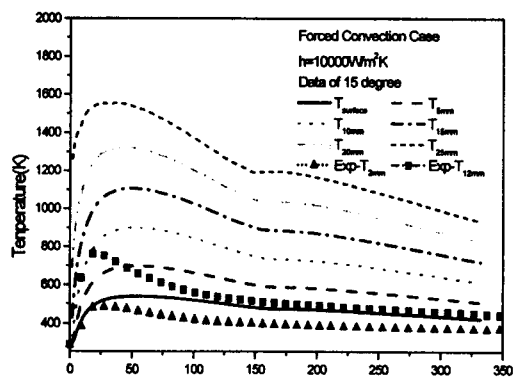

(b) h=10000 W/m²K

Fig. 14. Temperature Profile at 15° for Forced Convective Boiling

EXV experiment, we could not obtain the accurate bulk temperature. The error may have resulted from the following reason. Figure 14 shows the temperature profile for the region at 15°. When we assumed that the heat transfer coefficient was 5000 W/m²K, there was much difference between the computed results and the test data. But the difference was reduced for the case where the heat transfer coefficient was 10000 W/m²K. It appears that most likely there exists still unknown, very effective, turbulent eddy assisted heat transfer mechanism in the narrow hemispherical channel with expanding flow area inside the gap between the LAVA vessel and the COASISO structure (see Fig. 4). In this particular type geometry with downward facing heating no completely reliable theory is yet available in the literature. The remaining error existing in the vessel wall for the temperature profile was in most part due to the assumed initial temperature and the thermophysical properties of the thermite.

For the pool boiling, we investigated the same factors as the case of forced convective boiling as presented in Figs. 15 and 16. Different than the forced convective boiling, we could use the bulk temperature as the boundary condition. As the result of the sensitivity analysis for the heat transfer coefficient for the pool boiling, we could

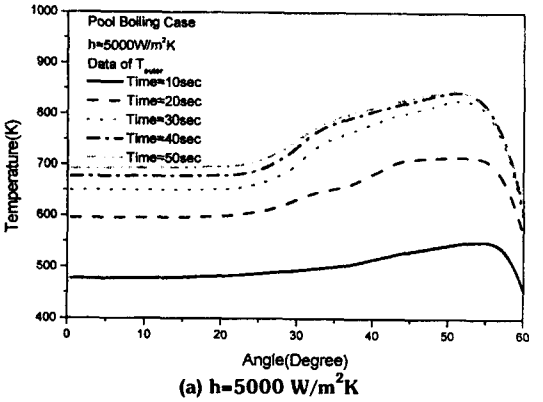

(a) h=5000 W/m²K

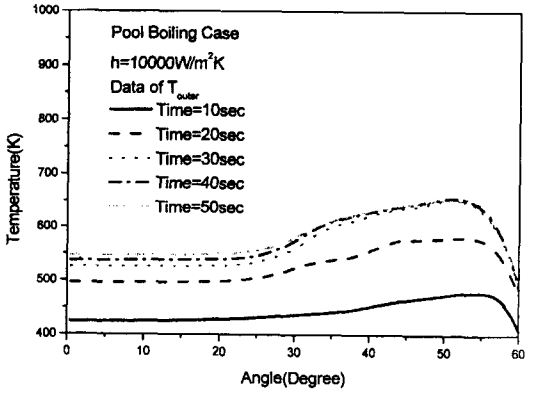

(b) h=10000 W/m²K

Fig. 15. Azimuthal Temperature Variation with Time for Pool Boiling

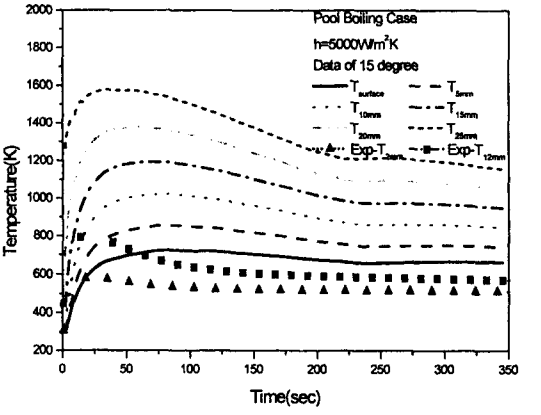

(a) h=5000 W/m²K

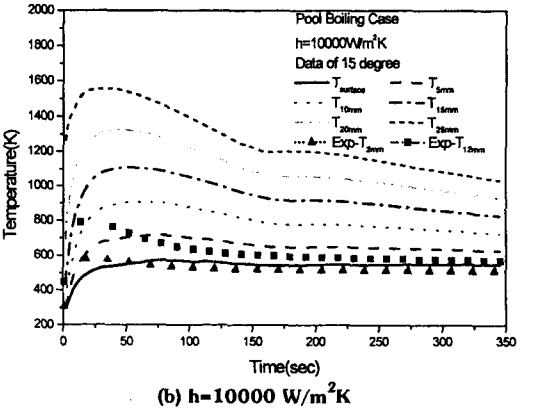

(b) h=10000 W/m²K

Fig. 16. Temperature Profile at 15° for Pool Boiling

surmise that the heat transfer coefficient should lie between 5000 W/m²K and 10000 W/m²K, which should be smaller than for the forced convective boiling. According to Yoon et al. [15], there were forced convection effect in the pool boiling by means of the buoyancy-driven two-phase flow boundary layer. It is thus surmised that the reason that the case of 10000 W/m²K was in closer agreement with the test data was most probably the two-phase boundary layer effect in the hemispherical annular gap, which greatly agitates.turbulent eddies to promote heat removal from the outer surface of the vessel.

5. Conclusions

In the scarcity of comprehensive predictive tool, a two-dimensional computational program was written to predict the temperature profile of a spherical vessel segment simultaneously accounting for the conjugate mechanisms of heat conduction through the debris and the vessel, natural convection heat transfer within the molten pool, and the ablation of the metallic vessel wall in contact with the high temperature melt. Results of the sensitivity analysis and comparison with the data from the LAVA-EXV experiment

demonstrated a high potential for our computational model to simulate thermal interactions of the RPV with the high temperature melt during a core melt accident. From this study it is concluded that the vessel wall ablation is the main parameter in addition to the natural convection effect during the process of assessing the RPV integrity as to the location of the hot spot and the time to possible failure. The simplistic natural convection model partly made up for the momentum equation not considered in this study. More rigorous thermal analysis may be made if the ablation and the natural convection effects are to be coupled with the momentum equation along with the energy equation in the computer program. Uncertainties in the prediction will also be reduced when more accurate initial and boundary conditions are supplied from the test in terms of material composition and its associated thermophysical properties.

Acknowledgement

The authors are grateful for the technical support from the Korea Atomic Energy Research Institute by providing with the LAVA-EXV experimental data and the FLUENT results.

Nomenclature

AL	left area of control volume
AD	down area of control volume
AR	right area of control volume
AU	upper area of control volume
c_p	specific heat at constant pressure
h_{air}	heat transfer coefficient of air
$h(\theta)$	azimuthal heat transfer coefficient
h_{down}	average heat transfer coefficient of the downward direction
k	thermal conductivity
r	radius
Δt	time step size
T	temperature
T_{bulk}	bulk temperature of cooling water
V	volume

Greek Letters

ε	emissivity
ϕ	polar angle at the pool surface
θ	angle along the vessel wall
ρ	density
σ	Stefan-Boltzmann constant

Superscripts

D	down
L	left
m	molten material
n	previous time step
n+1	present time step
R	right
U	upper
*	intermediate time step

Subscripts

abt	ablation
ini	initial
m	molten material
outer	outer surface
v	vessel

References

1. K. H. Kang et al., "A Feasibility Experiment for Assessing the Efficacy of Ex-Vessel Cooling through the External Gap Structure," Proc. of the Korean Nuclear Society Spring Meeting, Pohang, Korea, May 28-29 (1999).
2. J. E. O' Brien and G.L. Hawkes, "Thermal Analysis of a Reactor Lower Head with Core Relocation and External Boiling Heat Transfer," AIChE Symposium Series, 87, 283, 159 (1991).
3. H. J. Park and V. K. Dhir, "Effect of Outside

Cooling on the Thermal Behavior of a Pressurized Water Reactor Vessel Lower Head," *Nuclear Technology*, 100, 331 (1992).

4. F. Mayinger, M. Jahn, H. H. Reineke and U. Steinberner, "Examination of Thermohydraulic Process and Heat Transfer in a Core Melt," Final report BMFT RS 48/1, Technical University, Hannover, Germany (1975).
5. R. E. Henry et al., "Cooling of Core Debris within the Reactor Vessel Lower Head," *Nuclear Technology*, 101, 385 (1993).
6. Private Communication from K. H. Kang, Korea Atomic Energy Research Institute, to H. J. Yoon, Seoul National University, October (1999).
7. M. S. El-Genk et al., "Transient Heat Conduction During Quenching of Downward Facing Copper and Stainless Steel Convex Surfaces," *J. Numerical Heat Transfer* Part A, 29, 543 (1996).
8. H. J. Yoon and K. Y. Suh, "Sensitivity Studies on Thermal Margin of Reactor Vessel Lower Head During A Core Melt Accident," Proc. of the 8th International Conference on Nuclear Engineering (ICONE 8), Baltimore, MD, USA, April 2-6 (2000).
9. F. J. Asfia and V. K. Dhir, "An Experimental Study of Natural Convection in a Volumetrically Heated Spherical Pool with Rigid Wall," Int. Mechanical Engineering Congress & the Winter Annual Meeting, Chicago, IL, USA, November 6-11 (1994).
10. T. G. Theofanous et al., "In-vessel Coolability and Retention of a Core Melt," DOE/ID-10460, vol 1, U.S. Department of Energy, Washington, DC, USA (1995).
11. H. J. Park, V. K. Dhir and W. E. Kastenberg, "Effect of External Cooling on the Thermal Behavior of a Boiling Water Reactor Vessel Lower Head," *Nuclear Technology*, 108, 266-282 (1994).
12. K. Y. Suh and R. E. Henry, "Integral Analysis of Debris Material and Heat Transport in Reactor Vessel," *Nuclear Engineering and Design*, 151, 203-221 (1994).
13. M. Jahn and H. H. Reineke, "Free *Convection Heat Transfer with Internal Heat* Sources," Proc. of the Fifth Int. Heat Transfer Conference, 3, 74 (1974).
14. FLUENT 4.32 User's Guide, FLUENT Inc., Lebanon, NH, USA, January (1995).
15. H. J. Yoon K. Y. Suh and H. K. Kim, "Estimation of Thermal Margin for External Cooling of Lower Head," Trans. of the ANS Annual Meeting and Embedded Topical Meeting, Boston, MA, USA, June 6-10 (1999).